12-2013

A ferrofluid-based wireless pressure sensor

Girish Chitnis
Purdue University, Birck Nanotechnology Center, gchitnis@purdue.edu

Babak Ziaie
Purdue University, Birck Nanotechnology Center, bziaie@purdue.edu

Chitnis, Girish and Ziaie, Babak, "A ferrofluid-based wireless pressure sensor" (2013). *Birck and NCN Publications.* Paper 1550.
http://dx.doi.org/10.1088/0960-1317/23/12/125031

A ferrofluid-based wireless pressure sensor

2013 J. Micromech. Microeng. 23 125031

(http://iopscience.iop.org/0960-1317/23/12/125031)

J. Micromech. Microeng. **23** (2013) 125031 (6pp) doi:10.1088/0960-1317/23/12/125031

A ferrofluid-based wireless pressure sensor

Girish Chitnis[1,2] **and Babak Ziaie**[1,3]

[1] Birck Nanotechnology Center, Purdue University, West Lafayette, IN 47907, USA
[2] School of Mechanical Engineering, Purdue University, West Lafayette, IN 47907, USA
[3] School of Electrical and Computer Engineering, Purdue University, West Lafayette, IN 47907, USA

E-mail: gchitnis@purdue.edu

Received 19 August 2013, in final form 30 September 2013
Published 14 November 2013
Online at stacks.iop.org/JMM/23/125031

Abstract
This paper presents a wireless pressure sensor design based on magnetic fluid displacement over a planar coil and its corresponding inductance change. The design of the pressure sensor is presented followed by its fabrication and characterization. Experimental results show a good correlation with a nonlinear model relating the applied pressure to the change in coil self-resonant frequency. A prototype sensor (radius = 6 mm, thickness = 2 mm) based on the above principal using an oil-based ferrofluid (50 μl, ferrite concentration 2%), a polyimide-embedded planar coil ($L = 1$ μH), and a 25 μm thick polyimide membrane shows a sensitivity of 3 KHz mmHg^{-1} with a base-line resonant frequency of $f_0 = 109$ MHz.

(Some figures may appear in colour only in the online journal)

1. Introduction

Wireless sensing of physiological pressures has been an area of interest for more than half a century following the pioneering work of Mackay *et al* in 1957 to measure gastrointestinal pressure using an ingestible capsule containing a single transistor oscillator whose frequency was modulated by external pressure [1]. Later, in the 1960s, Collins [2] used a passive LC transponder to record intraocular pressure. These pioneering efforts were subsequently augmented with improvements in microfabrication and MEMS technology resulting in miniature devices designed to monitor pressures at various anatomical sites such as blood vessels [3, 4], eye [5–8], bladder [9], cranium [10], etc. Most such systems can be categorized as passive (comprising of a parallel LC circuit in which either the coil or the capacitor is pressure sensitive, thus allowing for remote monitoring of pressure by tracking the resonant frequency with an RF interrogator) or active (pressure sensor plus interface and RF electronics, powered through inductive methods or batteries). Although passive LC transponders are conceptually much less complicated than active systems, they frequently require fabrication of miniature capacitive pressure sensors with hermetic electrical feed-throughs, which is not a trivial task [11]. Here, we present a magneto-fluidic wireless pressure sensing technique which does not require a separate capacitor and is simple to implement. In this design, magnetic flux through the coil varies with applied pressure due to the transfer of trapped ferrofluid in the sensor, hence resulting in an inductance change. Since the coil itself has some built-in stray capacitances, no external capacitor is needed to create the LC tank (inductor self-resonant frequency is therefore a function of applied pressure). In addition to design, fabrication and characterization, Comsol^{TM} simulation is also performed to understand correlation between ferrofluid movements and inductance change.

2. Design

The working mechanism of the magneto-fluidic pressure sensor relies on magnetic permeability of colloidal ferrite nanoparticles and fluidity of the dispersion medium. Figure 1 shows the schematic diagram of the pressure sensor. The device consists of top and bottom chambers connected through a small hole and covered with thin polymeric membranes. The bottom chamber also incorporates a planar inductor. The small through-hole facilitates the transfer of ferrofluid between the two chambers. Figure 1(*a*) shows the device in its non-pressurized configuration, where all the ferrofluid is present in the top chamber. When pressure is applied on the top membrane, it transfers some of the ferrofluid closer to the coil, in the space created due to deflection of the bottom membrane,

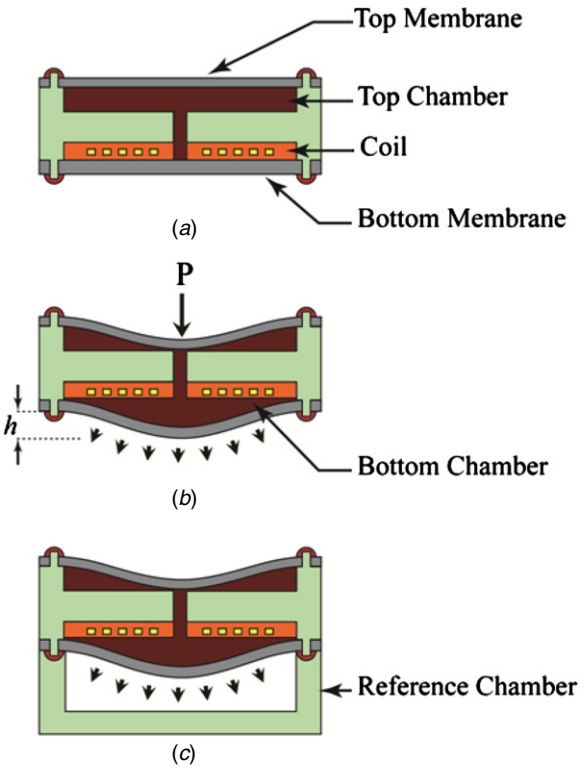

Figure 1. Schematic diagram of ferrofluid-based pressure sensor (dimensions not to scale).

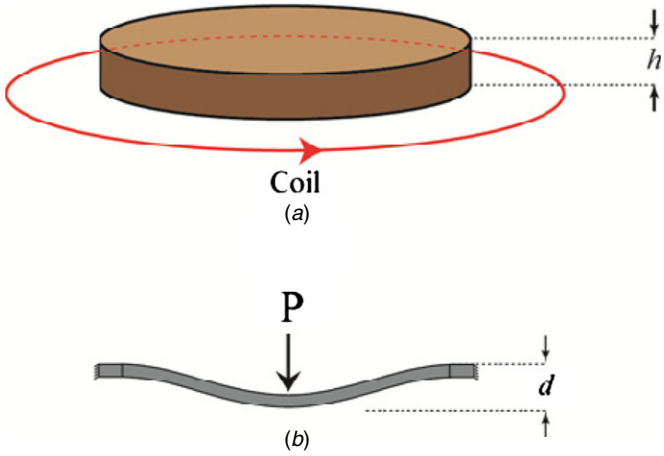

Figure 2. Parameters influencing the design of the ferrofluid-based pressure sensor.

as shown in figure 1(*b*). Since the magnetic permeability of ferrofluid is higher than that of polymeric membrane or surrounding air, it increases the inductance of the coil. Given that stray capacitance is unaffected by pressure variations, this leads to a drop in the self-resonant frequency of the coil as external pressure increases. A reference chamber can be added to measure absolute pressure, as shown in figure 1(*c*).

For a given pressure, the change in resonant frequency of the coil depends on the deflection of the polymeric membrane as well as the magnetic permeability of ferrofluid. For better understanding, a simplified geometry is shown (figure 2) in which a multi-turn spiral coil is represented as a single loop of wire. The volume of the ferrofluid closer to the coil is approximated as a cylindrical disc that changes its thickness (h) with applied pressure (figure 2(*a*)). Since this disc of ferrofluid is created due to the deformation of circular membrane, the thickness of the disc (h) is proportional to the deflection (d) of the circular membrane with clamped edges, figure 2(*b*). The inductance (L) of the coil increases as a function of thickness (h). Comsol^{TM} simulation is performed to study the effect of change in coil-inductance (L) with disc thickness (h). Figure 3(*a*) shows the coil geometry used in the simulation which is based on the final coil used for fabrication of the prototype. Inductance calculated from the simulation is plotted against disc thickness in figure 3(*b*). Based on these simulation results, we can assume that for a thin disc ($h \ll \rho_c$)

$$L = L_o + K_1' h, \tag{1}$$

where L_o = inductance of the coil in the absence of ferrofluid disc, K_1' = the proportionality constant, ρ_c = outer radius of the coil and h = thickness of the ferrofluid disc.

Change in resonant frequency for a small change in inductance can be derived from the basic formula of resonant frequency ($f = 1/2\pi\sqrt{\mathrm{LC}}$). This change can be expressed as change in inductance and original frequency, as shown in equation (2):

$$\Delta f = -f_o \cdot \frac{(L - L_o)}{2L_o}. \tag{2}$$

Substituting L from equation (1),

$$\Delta f = -\frac{f_o}{2L_o} \cdot K_1' h. \tag{3}$$

For a given configuration of pressure sensor, h is the only pressure-dependent variable. Hence, equation (3) can be represented as

$$\Delta f = -K_2' h \tag{4}$$

where K_2' is a new parametric constant that depends on the material properties and geometry of the device.

For a clamped circular membrane pressure, P, needed to achieve deflection, d, can be given as [12]

$$P = \frac{Et^3}{12(1-\nu^2)} \frac{64}{a^4} \left(d + \frac{0.488}{t^2} d^3 \right) \tag{5}$$

where a = radius of the membrane, E = elasticity of the material, t = thickness of the membrane, ν = Poisson's ratio and P = applied pressure.

The shape of ferrofluid accumulated under the deflected membrane can be approximated as a disc with thickness (h) proportional to the membrane deflection (d). With this approximation, and equations (4) and (5), we obtain the following expression relating applied pressure with the change in frequency:

$$P = -\frac{Et^3}{12(1-\nu^2)} \cdot \frac{64}{a^4} \cdot \left[\frac{\Delta f}{K_3'} + \frac{0.488}{t^2} \left(\frac{\Delta f}{K_3'} \right)^3 \right] \tag{6}$$

where K_3' is the new proportionality constant that incorporates K_2'. The equations presented here do not account for the residual stress present in the membrane which depends on the fabrication process of the device. However, we can conclude that the pressure and change in frequency are related through a cubic equation which can be represented as

$$P = -K_1 \Delta f - K_2 \Delta f^3 \tag{7}$$

where K_1 and K_2 are parametric constants based on the geometry and material properties.

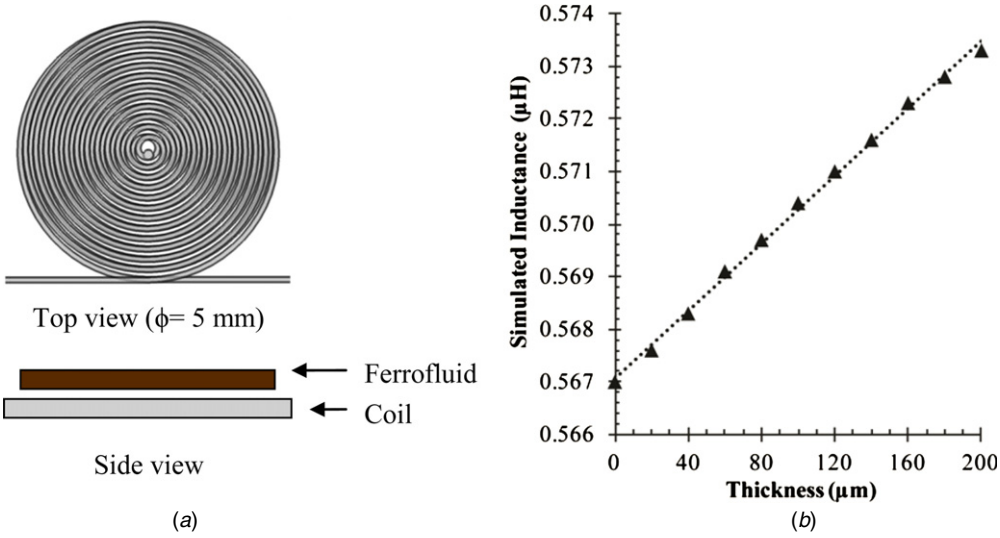

Figure 3. Comsol™ simulations. (*a*) Geometry of simulated coil and ferrofluid disc. (*b*) Simulated inductance versus ferrofluid disc thickness.

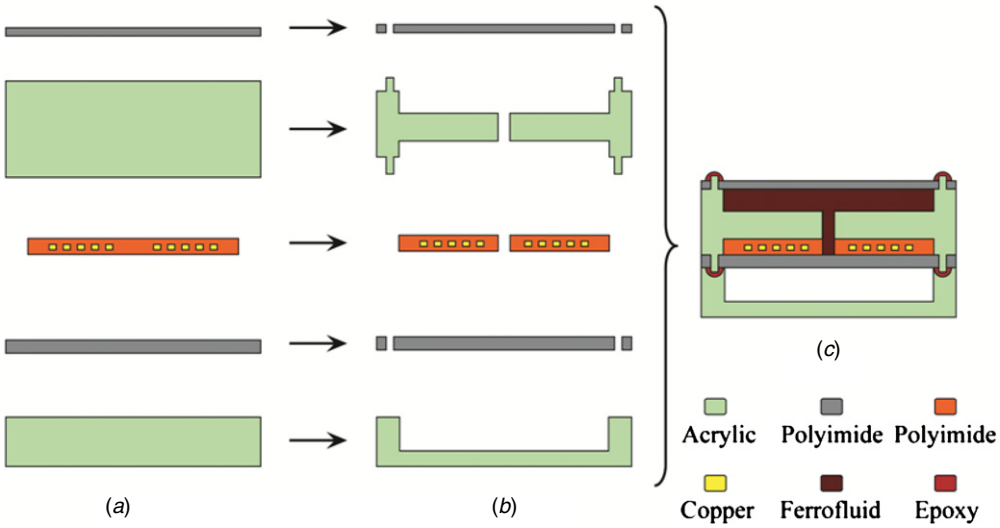

Figure 4. Fabrication process of ferrofluid-based pressure sensor.

3. Materials and methods

3.1. Device fabrication

Figure 4 shows the fabrication process sequence of the ferrofluid-based pressure sensor. Polyimide flexcoil ($L \approx 1\ \mu$H) is used for the fabrication of this prototype. The coil is designed in-house and fabricated by Parlex USA, Inc. It has 12 spiral turns of 18 μm thick copper (two layers) and 25 μm thick polyimide (three layers). A 25 μm thick polyimide sheet is used for both top and bottom polymeric membranes. The ferrofluid chamber and reference chamber are machined out of acrylic. All the machining is done using a CO_2 laser (Universal® Laser Systems), figure 4(*b*). After assembly, the top chamber is prefilled with ferrofluid (APG 311 by Ferrotec, Inc.) and then sealed using two-part epoxy resin, figure 4(*c*). One needs to be extremely careful not to trap any air bubbles while sealing the ferrofluid with the membranes. Air bubbles can move around the coil and lead to erratic readings. The ferrofluid has ferrite nanoparticles (volume concentration = 2%, particle size = 10 nm) dispersed in synthetic hydrocarbon with overall magnetic permeability of 1.1 (measured at f = 10 MHz). Table 1 lists important geometric parameters of the device. Figure 5 shows the photograph of the final fabricated prototypes. The one on the right shows a coil under polyimide membrane before filling the chamber with ferrofluid. When the ferrofluid is injected in the top chamber, a thin layer of the fluid also covers the coil, as shown in the completed device on the left in figure 5.

3.2. Measurements

The pressure sensor is characterized against a water column pressure as shown in figure 6. A sensor is mounted at the end of the tube connected to the water column with the coil facing the atmospheric pressure. Self-resonant frequency of the sensor is measured using a transceiver coil (single loop, ϕ = 12 mm) connected to an impedance analyzer using the

Figure 5. Optical photograph of fabricated prototype (device without ferrofluid on right and device with ferrofluid on left).

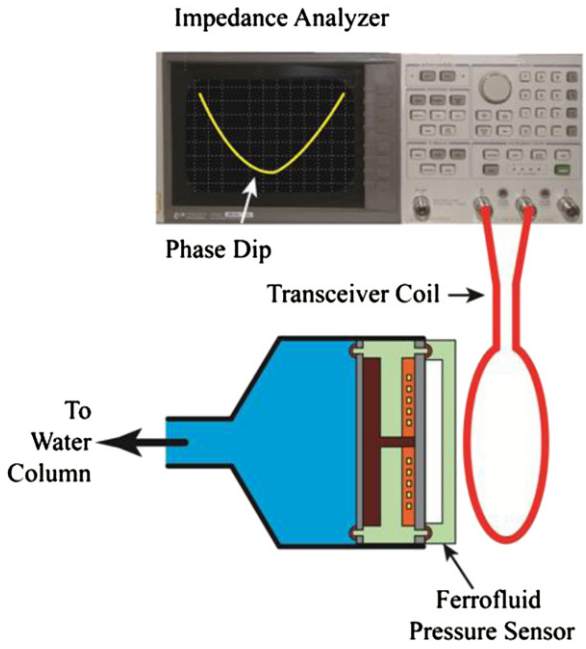

Figure 6. Schematic of the experimental setup.

Table 1. Ferrofluid pressure sensor parameters.

Ferrofluid pressure sensor	(mm)
Diameter	12
Thickness	2
Polyimide membrane	
Thickness	0.025
Diameter	–
Flexible	7
Total	12
Coil	
Thickness	0.250
Diameter	5
Hole size	
Diameter	1

phase-dip technique [13]. All the measurements are performed with the smallest distance possible between the sensor and coil. Phase of a circular loop is expected to be 90° but in proximity of an external inductor (the pressure sensor), it shows a dip in phase values and the location of minima corresponds to the resonant frequency of the external inductor. Resonant frequency is measured for pressures ranging from 0 to 60 mmHg while increasing and decreasing the pressure in steps of 5 mmHg.

4. Results and discussion

Figure 7(*a*) shows the data obtained from the network analyzer. As pressure is increased, phase-dip shifts to the left and reduces in size. The location of minimum frequency can be determined by curve fitting a polynomial through the data. Figure 7(*b*) shows the polynomial fit ($n = 3$) through the data. The location of the minimum phase in the polymeric fit is recorded as the resonant frequency of the sensor. Figure 8 shows the resonant frequencies plotted against applied pressure. Data points indicate the experimental values, whereas the dotted line is cubic fit corresponding to equation (6), with $K_1 = 267.4$ mmHg MHz^{-1} and $K_2 = 7812$ mmHg MHz^{-3}. Figure 9 shows the change in dip size as the sensor is moved away from the external coil. The dip is noticeable at the maximum distance of 6 mm which shows that the wireless range of the sensor is at least 6 mm which can be improved by optimizing the interrogation technique and the external receiver coil.

It is important to note that the sensor uses coil in open configuration. Since that is the only electrical component, no electrical connections are needed. One can fabricate such a coil with a single layer of metallization which simplifies fabrication significantly. Open coil configuration also makes the system electrically robust. A broken connection in an open coil might result in an inductor with a different set of properties and alter the sensitivity, but it can still function as a pressure sensor. Although biocompatibility of the device in its current form is not validated, a conformal coating of parylene can be applied to ensure biological inertness. Further, the design is not material-specific; therefore, the structural components (acrylic chamber, polyimide membrane) can be easily replaced with more biocompatible materials. The only irreplaceable component, ferrite nanoparticles, is shown to be biocompatible [14, 15], and it has been proposed as an implant for the treatment of retinal detachment [16].

Although the use of high permeability material in the form of fluid (i.e. ferrofluid) facilitates easy transfer from one chamber to the other, it also has some disadvantages. In the current design, ferrofluid is in direct contact with the deflecting membranes. This increases damping significantly which reduces the resonant frequency and hence adversely affects the response time. Further, the fluid needs to move from one chamber to the other which also adds significant delay between pressure application and change in inductance. Therefore, the sensor will not perform well if fast measurements are necessary. Time response can be improved by using ferrofluid with lower viscosity, smaller chamber and larger hole for the fluid transfer. Increasing the radius of the membrane can lead to better sensitivity but it also needs more fluid to be transferred which leads to increase in response time.

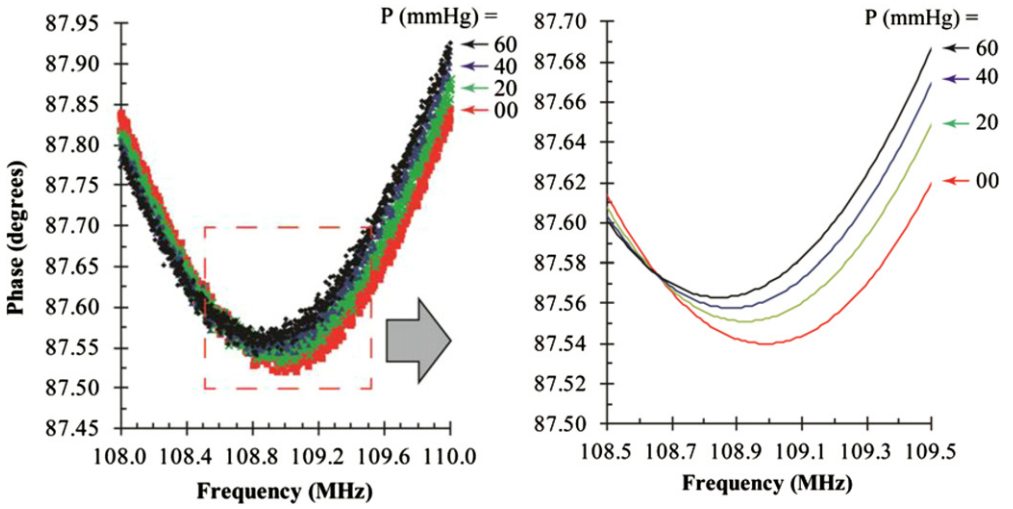

Figure 7. (*a*) Raw data obtained from network analyzer and (*b*) polynomial fit line (order = 3) through the data.

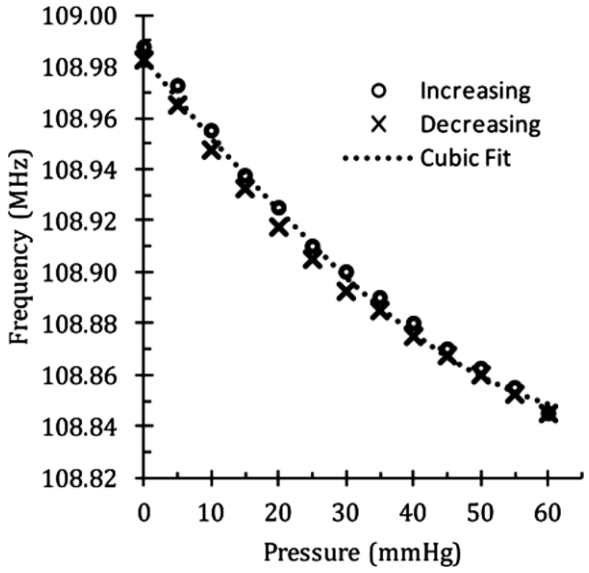

Figure 8. Sensor self-resonant frequency versus pressure.

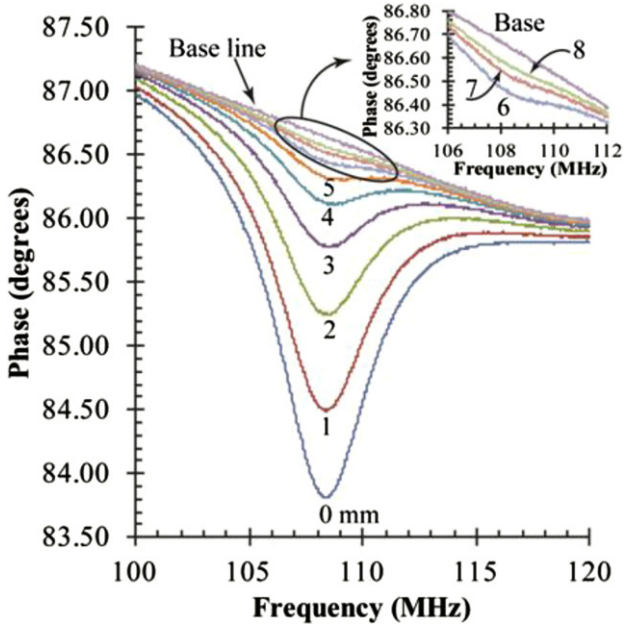

Figure 9. Variation in dip size with distance between the sensor and external coil (number under each curve shows the distance between sensor and external coil in millimeters).

Resonant frequency of the sensor is also a function of temperature. If the thermal coefficient of expansion of ferrofluid is higher than the material used to build the chamber, it will lead to bulging of membranes and hence increase the inductance of the sensor. Similarly, inductance will reduce with temperature if opposite is true. However, chamber material and carrier fluid for the ferrofluid can be chosen carefully to minimize temperature sensitivity. Further, as a biomedical implantable sensor, one can expect the environmental temperature to have minor variations. The effect of fatigue and creep also needs to be considered for long stability of the sensor. Although polymer is easy to machine, it can creep under constant pressure which can cause sensor drift. Metallic or glass membranes perform better than polymeric ones for long-term usage. However, metallic membrane will interfere with the wireless readout, whereas glass is difficult to machine. Hence, choice of glass versus polymer will depend on the specific application.

5. Conclusions

In this paper, we discussed a new pressure sensing technique based on magnetic liquid displacement and corresponding inductance change. Comsol^{TM} simulation is performed to understand the effect of ferrofluid on the inductance of the coil for a thin disc inductance varies linearly with the thickness. A pressure sensor is designed, fabricated and tested *in vitro*. The sensor shows a sensitivity of 3 KHz mmHg^{-1} (f_0 = 109 MHz) and wireless range of 5 mm. Sensitivity of the device can be further improved by optimizing geometric parameters and material properties, whereas the interrogation technique needs to be improved to increase the range.

References

[1] Mackay R S and Jacobson B 1957 Endoradiosonde *Nature* **179** 1239–40

[2] Collins C C 1967 Miniature passive pressure transensor for implanting in the eye *IEEE Trans. Biomed. Eng.* **14** 74–83

[3] Allen M G 2005 Micromachined endovascularly-implantable wireless aneurysm pressure sensors: from concept to clinic *Transducers'05: Proc.13th Int. Conf. on Solid-State Sensors, Actuators and Microsystems* vol 1 pp 275–8

[4] Ziaie B and Najafi K 2001 An implantable microsystem for tonometric blood pressure measurement *Biomed. Microdevices* **3** 285–92

[5] Eggers T *et al* 2000 Wireless intra-ocular pressure monitoring system integrated into an artificial lens *EMBS: Proc. 1st Annu. Int. IEEE Special Topic Conf. on Microtechnologies in Medicine and Biology* pp 466–9

[6] Stangel K, Kolnsberg S, Hammerschmidt D, Hosticka B, Trieu H and Mokwa W 2001 A programmable intraocular CMOS pressure sensor system implant *IEEE J. Solid-State Circuits* **36** 1094–100

[7] Rodger D C, Saati S and Humayun M S 2008 Microfabricated implantable parylene-based wireless passive intraocular pressure sensors *J. Microelectromech. Syst.* **17** 1342–51

[8] Chitnis G, Maleki T, Samuels B, Cantor L B and Ziaie B 2013 A minimally invasive implantable wireless pressure sensor for continuous IOP monitoring *IEEE Trans. Biomed. Eng.* **60** 250–6

[9] Melgaard J and Rijkhoff N J M 2011 Detecting the onset of urinary bladder contractions using an implantable pressure sensor *IEEE Trans. Neural Syst. Rehabil. Eng.* **19** 700–8

[10] Ghannad-Rezaie M, Yang L J-S, Garton H J L and Chronis N 2012 A near-infrared optomechanical intracranial pressure microsensor *J. Microelectromech. Syst.* **21** 23–33

[11] Haque R and Wise K 2011 A 3D implantable microsystem for intraocular pressure monitoring using a glass-in-silicon reflow process *MEMS'11: Proc. 24th Int. Conf. on Micro Electro Mechanical Systems* pp 995–8

[12] Timoshenko S and Woinowsky-Krieger S 1959 *Theory of Thin Plates and Shells* 2nd edn (New York: McGraw-Hill)

[13] Akar O, Akin T and Najafi K 2001 A wireless batch sealed absolute capacitive pressure sensor *Sensors Actuators A* **95** 29–38

[14] Tomitaka A, Hirukawa A, Yamada T, Morishita S and Takemura Y 2009 Biocompatibility of various ferrite nanoparticles evaluated by *in vitro* cytotoxicity assays using HeLa cells *J. Magn. Magn. Mater.* **321** 1482–4

[15] Kim D-H, Lee S-H, Kim K-N, Kim K-M, Shim I-B and Lee Y-K 2005 Cytotoxicity of ferrite particles by MTT and agar diffusion methods for hyperthermic application *J. Magn. Magn. Mater.* **293** 287–92

[16] Mefford O T *et al* 2007 Field-induced motion of ferrofluids through immiscible viscous media: testbed for restorative treatment of retinal detachment *J. Magn. Magn. Mater.* **311** 347–53